A biliverdin-binding cyanobacteriochrome from the chlorophyll d–bearing cyanobacterium Acaryochloris marina

SCIENTIFIC REPORTS

OPEN

SUBJECT AREAS:
PROTEINS
LIGHT RESPONSES

Received
31 October 2014

Accepted
22 December 2014

Published
22 January 2015

Correspondence and requests for materials should be addressed to R.N. (narikawa.rei@shizuoka.ac.jp)

A biliverdin-binding cyanobacteriochrome from the chlorophyll *d*–bearing cyanobacterium *Acaryochloris marina*

Rei Narikawa[1,2,3], Takahiro Nakajima[2], Yuki Aono[2], Keiji Fushimi[1], Gen Enomoto[2], Ni-Ni-Win[2], Shigeru Itoh[4], Moritoshi Sato[2] & Masahiko Ikeuchi[2,5]

[1]Department of Biological Science, Faculty of Science, Shizuoka University, Ohya, Suruga-ku, Shizuoka 422-8529, Japan, [2]Graduate School of Art and Sciences, University of Tokyo, Komaba, Meguro, Tokyo 153-8902, Japan, [3]Precursory Research for Embryonic Science and Technology, Japan Science and Technology Agency, 4-1-8 Honcho Kawaguchi, Saitama 332-0012 Japan, [4]Division of Material Science, Graduate School of Science, Nagoya University, Nagoya 464-8602, Japan, [5]Core Research for Evolutional Science and Technology, Japan Science and Technology Agency, 4-1-8 Honcho Kawaguchi, Saitama 332-0012 Japan.

Cyanobacteriochromes (CBCRs) are linear tetrapyrrole-binding photoreceptors in cyanobacteria that absorb visible and near-ultraviolet light. CBCRs are divided into two types based on the type of chromophore they contain: phycocyanobilin (PCB) or phycoviolobilin (PVB). PCB-binding CBCRs reversibly photoconvert at relatively long wavelengths, i.e., the blue-to-red region, whereas PVB-binding CBCRs reversibly photoconvert at shorter wavelengths, i.e., the near-ultraviolet to green region. Notably, prior to this report, CBCRs containing biliverdin (BV), which absorbs at longer wavelengths than do PCB and PVB, have not been found. Herein, we report that the typical red/green CBCR AM1_1557 from the chlorophyll *d*–bearing cyanobacterium *Acaryochloris marina* can bind BV almost comparable to PCB. This BV-bound holoprotein reversibly photoconverts between a far red light–absorbing form (Pfr, λmax = 697 nm) and an orange light–absorbing form (Po, λmax = 622 nm). At room temperature, Pfr fluoresces with a maximum at 730 nm. These spectral features are red-shifted by 48∼77 nm compared with those of the PCB-bound domain. Because the absorbance of chlorophyll *d* is red-shifted compared with that of chlorophyll *a*, the BV-bound AM1_1557 may be a physiologically relevant feature of *A. marina* and is potentially useful as an optogenetic switch and/or fluorescence imager.

Cyanobacteriochromes (CBCRs) are linear tetrapyrrole-binding photoreceptor proteins that are distantly related to red/far-red light–absorbing, bilin-chromophore containing phytochromes found in plants and certain bacteria and spectrally diverse as they absorb light in the near-ultraviolet and visible regions[1–12]. For CBCRs, their GAF (cGMP-phosphodiesterase/adenylate cyclase/FhlA) domains are the only type of domain necessary for chromophore binding and photoconversion, whereas phytochromes require PAS (Per/Arnt/Sim), GAF, and PHY (phytochrome-specific) domains. A canonical Cys within a CBCR GAF domain covalently binds a linear tetrapyrrole chromophore at ring A (Fig. 1*A, B*). A *Z*/*E* isomerization of the C15=C16 double bond between rings C and D of the tetrapyrrole moiety occurs during photoconversion. Certain CBCRs are involved in photo-acclimation processes, e.g., regulation of the chromatic acclimation of phycobiliproteins, regulation of phototactic orientation of cells, and light-dependent cell aggregation[5,13–16]. The spectral diversity of CBCRs is a consequence of the specific type of chromophore and the specific color-tuning mechanism used, i.e., reversible ligation of a second Cys to the chromophore[1,6,17,18] or a chromophore protonation/deprotonation cycle[19].

CBCRs are roughly divided into two types based on their chromophore: phycoviolobilin (PVB) and phycocyanobilin (PCB, Fig. 1*A*). PVB-binding CBCRs reversibly photoconvert at relatively short wavelengths, i.e., near-ultraviolet-to-green light[3,4,6,10,11,14]. PCB-binding CBCRs reversibly photoconvert at relatively long wavelengths, i.e., blue-to-red light[1,2,8,9,19,20]. Certain PCB-binding CBCRs are defined as red/green and green/red types. The red/green types photoconvert between a red light–absorbing thermostable state (Pr; C15-*Z* PCB) and a green light–

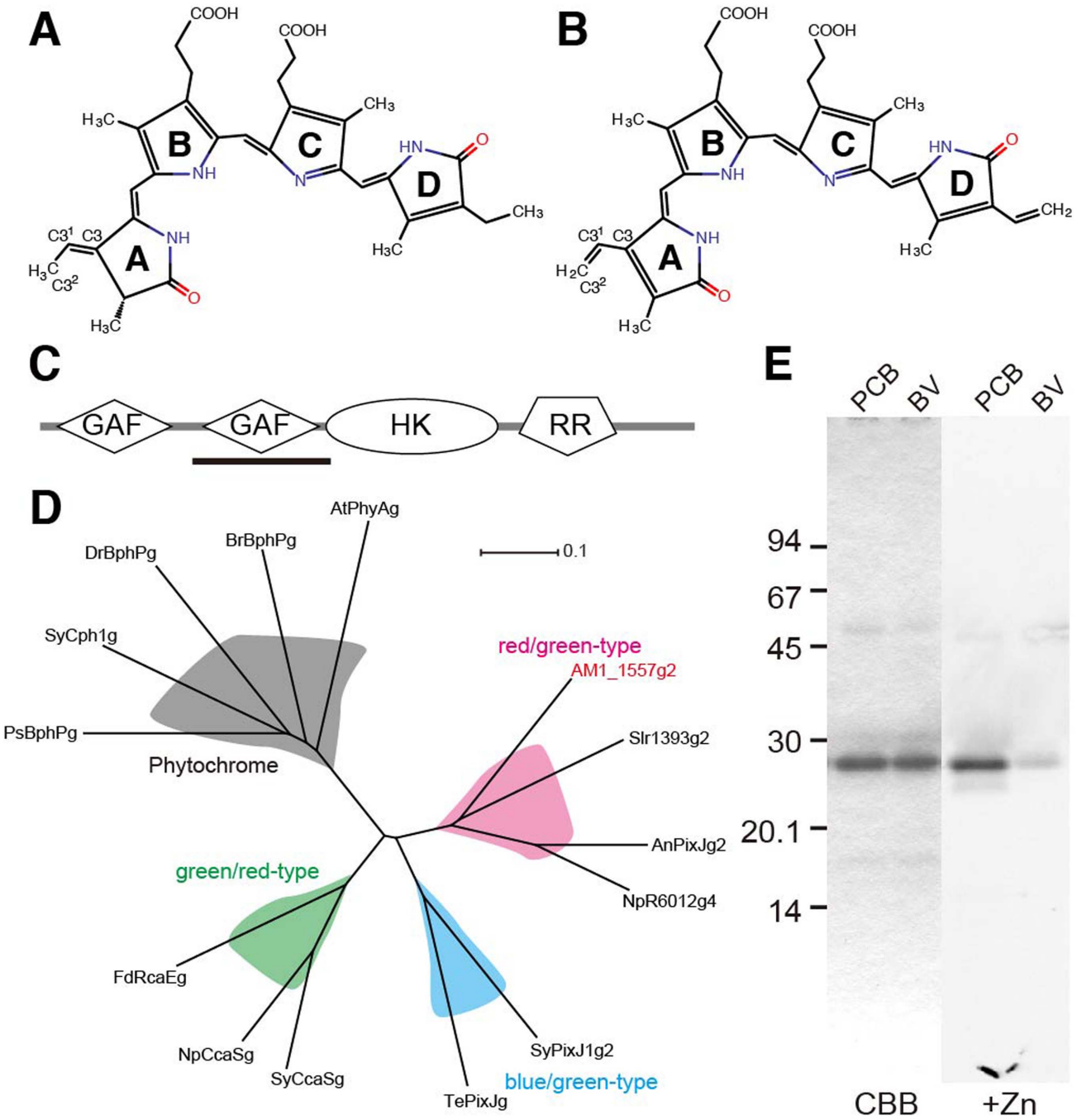

Figure 1 | Chromophores and AM1_1557. Chemical structures of (*A*) PCB and (*B*) BV. (*C*) Domain architecture of AM1_1557 according to a SMART motif analysis. (*D*) Cluster analysis of red/green, green/red, and blue/green CBCR and phytochrome GAF domains. The position of AM1_1557g2 on the tree is highlighted in red. (*E*), His-tagged AM1_1557g2-PCB (PCB) and AM1_1557g2-BV (BV) purified from PCB- and BV-producing *E. coli*, respectively (2 μg protein per gel lane). Coomassie brilliant blue (CBB)-stained gel and in-gel Zn-dependent fluorescence assay (+Zn).

absorbing metastable state (Pg; C15-*E* PCB)[8,20–24], whereas the green/red types photoconvert between a green light–absorbing thermostable state (Pg; C15-*Z* PCB) and a red light–absorbing metastable state (Pr; C15-*E* PCB).

We recently determined the crystal structure of the red/green CBCR AnPixJg2 Pr and found that its chromophore and tertiary structure are quite similar to those of phytochrome Pr, although the detailed chromophore-protein interaction is distinctive[25,26]. Conversely, the green light–absorbing mechanism of AnPixJg2 must be quite different from that of the far-red light–absorbing mechanism of phytochromes. Although hydration and ring D distortion may occur during photoconversion, their color-tuning mechanisms remain unclear[25,27]. For green/red CBCRs, color tuning depends on PCB protonation in Pr and deprotonation in Pg, irrespective of the C15-*Z*/*E* configuration[19].

CBCRs have been found only in cyanobacteria. Although cyanobacteria form a monophyletic clade, they have extensively diversified morphology, habitats, and photosynthetic properties. Among them, *Acaryochloris marina* is unique with respect to its photosynthetic pigments[28,29]. As its photosynthetic pigment, *A. marina* contains chlorophyll (Chl) *d*—which has an absorbance maximum at ~710 nm—instead of Chl *a*—which has an absorbance maximum at ~675 nm. Photochemical reaction center pigments for photosystem II and photosystem I, P680 and P700, in more typical cyano-

bacteria are substituted by P713 and P740, respectively, in *A. marina*[30,31]. *A. marina* produces Chl *d*-binding photosynthetic antenna complexes[32], such that *A. marina* uses red-shifted light sources for photosynthesis, which normal cyanobacteria and algae do not. Given these observations, we hypothesized that *A. marina* might also possess CBCR photoreceptors in its genome[33] that absorb light of longer wavelengths than do typical cyanobacteria.

Optogenetics and bio-imaging are now powerful techniques for regulating and monitoring cellular activities, and so various light-absorbing proteins are applied to these techniques[34]. Particularly, proteins absorbing long-wavelength light are needed for penetration to animal tissues[35]. In this context, it is meaningful to discover or artificially synthesize CBCRs that absorb long-wavelength light. Here, we focused on biliverdin (BV, Fig. 1*B*) chromophore that absorbs longer wavelength light than PCB. BV has been reported to covalently ligate to bacterial phytochromes (Bphs) but not to known CBCRs[36,37]. The non-photoconvertible long wavelength form of CBCR is suitable for the stable fluorescent probe. We selected red/green CBCR to look for BV-binding, because its Pr form is a thermostable form.

We report herein that a recombinant red/green CBCR from *A. marina* MBIC11017 effectively binds BV to form a photoreversible complex that absorbs and fluoresces at longer wavelengths than does the PCB-binding complex, suggesting that it may be relevant to far-red light-responsive feature of *A. marina* and suitable as an optogenetic switch or fluorescent imaging tool.

Results

Sequence Characteristics of AM1_1557g2. AM1_1557 is a typical bacterial two-component signal-transduction protein of 883 amino acid residues, two GAF domains, one His kinase (HK) domain, and one response regulator (RR) domain (Fig. 1*C*). The second GAF domain (AM1_1557g2, residues 220–364) is a red/green CBCR according to our sequence alignment (Fig. S1) and cluster analysis (Fig. 1*D*). Its sequence has 50% residue identity with that of AnPixJg2 and contains residues that are highly conserved in red/green CBCRs, i.e., Trp272, Asp274, and Tyr335 (Fig. S1).

Photoconversion of AM1_1557g2-PCB and –BV. AM1_1557g2 expressed in a PCB- or BV-producing *E. coli* was purified to near homogeneity (Fig. 1*E*, CBB). PCB and BV covalently bound AM1_1557g2 judging from the Zn-dependent fluorescence assay (Fig. 1*E*, +Zn). AM1_1557g2-PCB reversibly photoconverts between a red light–absorbing form (Pr; absorbance maximum, 649 nm) and a green light–absorbing form (Pg; absorbance maximum, 545 nm; Fig. 2*A*). This photoconversion is quite similar to that of AnPixJg2, a typical red/green CBCR[8]. The blue-pink color change of a solution of AM1_1557g2-PCB is clearly seen (Fig. 2*G*). Conversely, AM1_1557g2-BV reversibly photoconverts between a far-red light–absorbing form (Pfr; absorbance maximum, 697 nm) and an orange light–absorbing form (Po, absorbance maximum, 622 nm; Fig. 2*B*). The green-blue color change of a solution of AM1_1557g2-BV is also clearly seen (Fig. 2*H*). The absorbance maxima of AM1_1557g2-BV Pfr and Po are 48- and 77-nm red-shifted compared with those of AM1_1557g2-PCB Pr and Pg. The (Pfr – Po) difference spectrum has maxima at 699 and 378 nm, and a minimum at 606 nm, whereas the (Pr – Pg) difference spectrum has maxima at 649 and 351 nm, and a minimum at 540 nm (Fig. 2*C*). Because the maximum absorbances of free BV and PCB in solution are at 670 and 610 nm, respectively[38], the difference in the absorbance maxima of the two AM1_1557g2 forms roughly corresponds to the difference in the absorbances of the free chromophores. Isosbestic points are present in spectra recorded during the photoconversion processes of AM1_1557g2-PCB (584 and 449 nm) and AM1_1557g2-BV (652 and 480 nm), indicating no noticeable heterogeneity or intermediates (Fig. 3). Further, photoconversion could be repeated many times without appreciable deterioration of the spectra.

Chromophore Species, Their Configurations and Dark Reversion Kinetics. To conclusively identify the chromophore species and their configurations, spectra were obtained for acid-denatured AM1_1557g2-PCB and -BV. Absorption maxima of denatured AM1_1557g2-PCB Pr and Pg were observed at ~664 and ~594 nm, respectively (Fig. 2*D*, Fig. S2). Absorption maxima of denatured AM1_1557g2-BV Pfr and Po were observed at ~700 and ~620 nm, respectively (Fig. 2*E*, Fig. S2). These absorbance maxima of AM1_1557g2-BV Pfr and Po forms are about 50–60 nm red-shifted compared to those of AM1_1557g2-PCB Pr and Pg forms. Irradiation of denatured Pg and Po with white light resulted in red shift of the absorption spectra (Fig. S3). Further, the spectral difference between denatured AM1_1557g2-BV Pfr and Po forms is identical to those of denatured PaBphP-BV (bacterial phytochrome that covalently binds BV from *Pseudomonas aeruginosa*) Pfr and Pr forms (Fig. S4)[39], indicating that AM1_1557g2 Pfr is the thermostable state containing 15*Z*-BV, whereas its metastable state is Po containing 15*E*-BV. In terms of their chromophore configurations, AM1_1557g2-BV Pfr and Po correspond to AM1_1557g2-PCB Pr and Pg, respectively. We measured dark reversion kinetics of the thermostable states at room temperature. Unexpectedly, AM1_1557g2-PCB showed very slow dark reversion with half-life of 93 hours, whereas AM1_1557g2-BV showed quick dark reversion with half-life of 1 hour (Fig. 4).

Covalent Attachment of BV to AM1_1557g2 via Cys304. Recently, we solved the crystal structure of AnPixJg2 Pr in which Cys321 within its GAF domain is ligated to PCB C3[1] (Fig. S5)[25]. Our Zn-blot study indicates that AM1_1557g2 is covalently bound to BV (Fig. 1*E*). AnPixJg2 Cys321 corresponds to AM1_1557g2 Cys304 according to our sequence alignment (Fig. S1). To show that AM1_1557g2 Cys304 is covalently bound to the chromophore, we prepared the mutant C304A with an Ala substituted for Cys304. The Zn blot of C304A indicated that BV was not covalent bound to C304A (Fig. 5*A*). In addition, C304A did not absorb visible light (Fig. 5*B*). These results strongly indicate that AM1_1557g2 covalently binds BV via Cys304. This is the first report showing that the conserved CBCR GAF Cys can covalently ligate BV.

Fluorescence Spectroscopy. Room temperature fluorescence spectra of the thermostable states, AM1_1557g2-PCB Pr and -BV Pfr, were measured to evaluate their potential as fluorescence imagers. AM1_1557g2-BV Pfr fluoresces with a maximum at 730 nm, whereas AM1_1557g2-PCB Pr fluoresces with a maximum at 676 nm (Fig. 6). The fluorescence maximum of AM1_1557g2-BV Pfr is red-shifted by 54 nm compared with that of AM1_1557g2-PCB, a red shift quite similar to that found for their absorption spectra maxima. Fluorescence quantum yields of the Pr and Pfr form were 1.7% and 0.3%.

The fluorescence of AM1_1557g2-PCB, AM1_1557g2-BV, and free PCB and BV were directly observed under a fluorescence stereomicroscope. AM1_1557g2-PCB Pr intensely fluoresced, whereas free PCB did not (Fig. 7*A and B*). In addition, we detected a change in fluorescent intensity from Pr during the photoconversion of Pr and Pg (Fig. 7*C* and Movie S1). The solution of AM1_1557g2-PCB was constantly red-light irradiated, resulting in photoconversion of Pr to Pg concomitant with a fluorescence decrease to almost the background level. Upon green light irradiation Pg photoconverted to Pr, and the fluorescence largely increased.

Similarly, the fluorescence of AM1_1557g2-BV Pfr, but not that of free BV, was clearly observed (Fig. 7*D and E*). In addition, we detected a change in fluorescence intensity from Pfr during the Pfr to Po photoconversion (Fig. 7*F* and Movie S2). The solution of AM1_1557g2-BV was constantly irradiated with far-red light (FRL, 710/75 nm), resulting in photoconversion of Pfr to Po con-

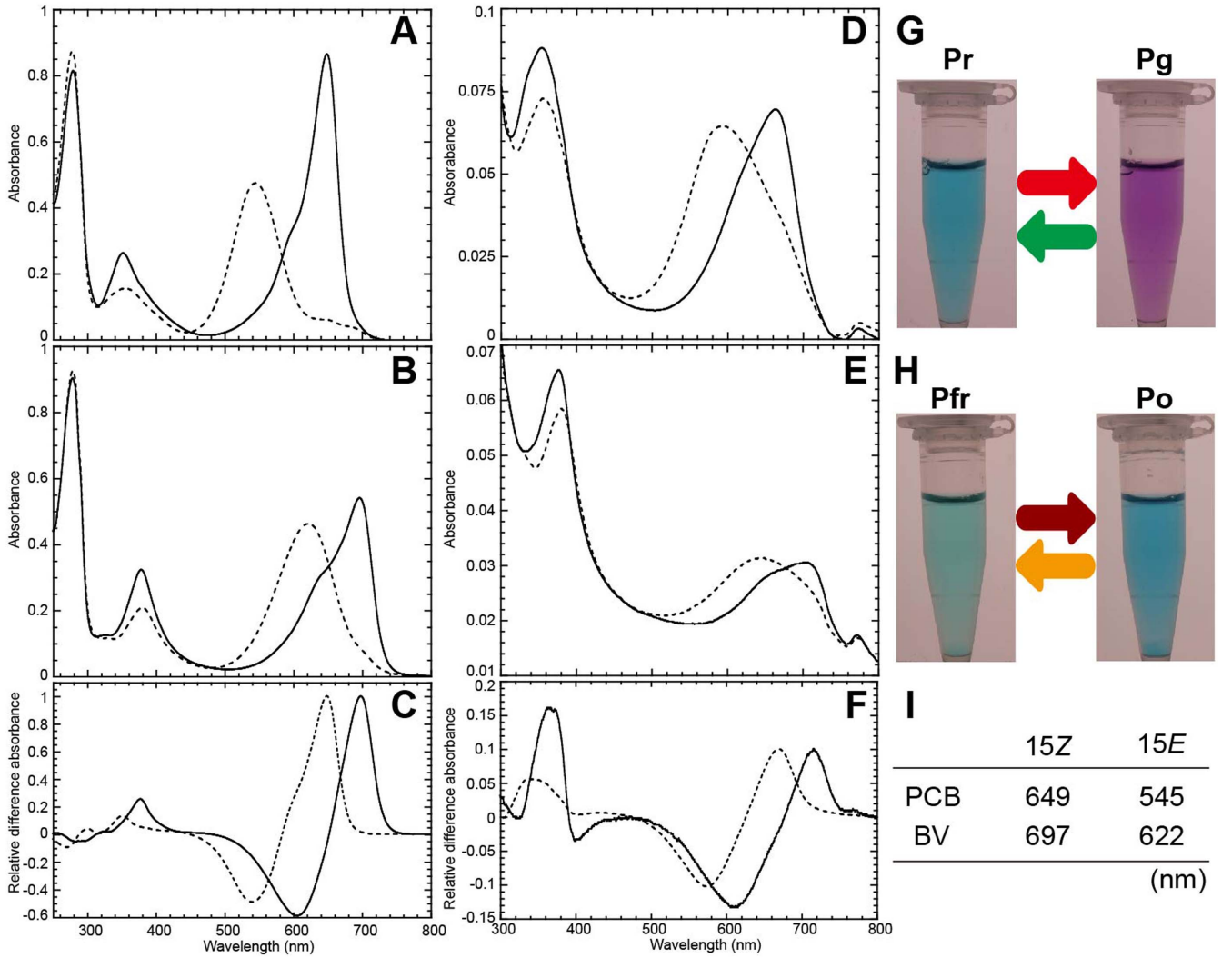

Figure 2 | Reversible photoconversion of AM1_1557g2-PCB and AM1_1557g2-BV. (*A*) Absorbance spectra of native AM1_1557g2-PCB Pr (solid line) and Pg (broken line). (*B*) Absorbance spectra of native AM1_1557g2-BV Pfr (solid line) and Po (broken line). (*C*), Difference spectra of native AM1_157g2-PCB (Pr – Pg; broken line) and native AM1_1557g2-BV (Pfr – Po; solid line). (*D*) Absorbance spectra of acid-denatured AM1_1557g2-PCB Pr (solid line) and Pg (broken line). (*E*) Absorbance spectra of acid-denatured AM1_1557g2-BV Pfr (solid line) and Po (broken line). (*F*) Difference spectra of acid-denatured AM1_1557g2-PCB (Pr – Pg; broken line) and acid-denatured AM1_1557g2-BV (Pfr – Po; solid line). (*G*) Color change of a solution of AM1_1557g2-PCB upon irradiation with red or green light. (*H*) Color change of a solution of AM1_1557g2-BV upon irradiation with far-red or orange light. (*I*) Wavelength maxima of the 15*Z* and 15*E* forms of AM1_1557g2-PCB and AM1_1557g2-BV.

comitant with a decrease in fluorescence. When irradiated with orange light, Po photoconverted to Pfr, and the fluorescence largely increased. The Pfr fluorescence was not completely abolished by far-red irradiation possibly due to incomplete photoconversion. Thus, irradiation by red-shifted far-red light (FRL-2, 720/40 nm) further decreased its fluorescence (Fig. S6 and Movie S3). In both cases, photoconversion was almost complete within 1 min and repetitive photoconversion did not affect the cyclic increase and decrease of fluorescence intensity (Fig. 7*C and F*).

Discussion

In this study, we prepared the BV-binding CBCR GAF domain, AM1_1557g2-BV, which is the first time a CBCR GAF domain has been shown to bind BV. AM1_1557g2 efficiently binds BV via the canonical GAF Cys304 and reversibly photoconverts in its BV form between Pfr with an absorbance maximum at 697 nm and Po with an absorbance maximum at 622 nm. Furthermore, at room temperature, Pfr fluoresces with a maximum at 730 nm. These experiments suggest that AM1_1557 binds BV in vivo, which would make it highly useful as an optogenetic switch and/or fluorescent imaging tool.

A. marina is unusual cyanobacterium, in that it possesses Chl *d*, instead of Chl *a*, as its main photosynthetic pigment. Chl *d* absorbs light at ~710 nm, whereas Chl *a* absorbs light at ~675 nm, suggesting that for effective photosynthesis *A. marina* may need to absorb light of longer wavelengths than do cyanobacteria that possess only Chl *a*. Because the maximum absorbance of BV is red-shifted by ~60 nm compared with that of PCB, we hypothesized that *A. marina* may also possess a CBCR(s) that can bind BV instead of PCB to sense light of longer wavelengths. We therefore focused on the red/green CBCR, selected AM1_1557 from *A. marina* because its GAF domain is highly similar to the representative AnPixJg2, and obtained the recombinant BV-binding GAF domain, AM1_1557g2.

Here, we estimated binding efficiency of BV to AM1_1557g2 in comparison with that of PCB based on fluorescence intensities on SDS-PAGE gel (Fig. 1E), native protein absorptions (Fig. 2A and B) and denatured protein absorptions (Fig. 2D and E) that are standardized by free PCB and BV data (Fig. S7). By these three different

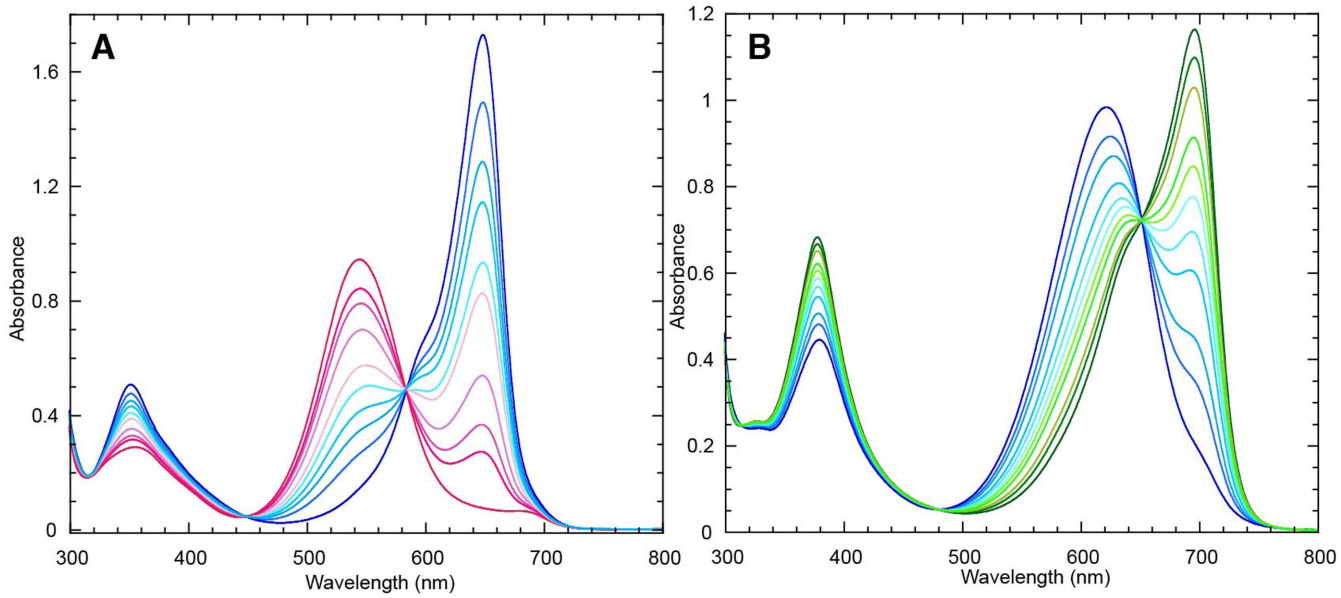

Figure 3 | Presence of isosbestic points in the spectra of AM1_1557g2-PCB and -BV obtained during photoconversion. (*A*) Absorption spectra AM1_1557g2-PCB acquired during its (Pr – Pg) photoconversion. (*B*) Absorption spectra of AM1_1557g2-BV acquired during its (Pfr – Po) photoconversion. Spectral measurements after irradiation with light intensity of 100 μmol $m^{-2}s^{-1}$ for approximately 3-to-30 s were performed and representative spectra are shown.

calculations, the binding efficiency of BV was estimated at approximately 55% (52–57%) in comparison with PCB.

Because the structure of BV differs from that of PCB at C18 (an ethylidene vs. a vinyl moiety, respectively) and at ring A, which covalently binds to the apoprotein (Fig. 1*A and B*), it is somewhat surprising that the two chromophores bind AM1_1557g2 similarly. Specifically, the difference in the ring A substituents has been assumed to be critical for chromophore selectivity. Crystal structures of Bph-BV[40], and Cph1-[41] and CBCR-PCBs[25] clearly show different orientations of the canonical Cys-ring A covalent bond, which may reflect different positional reactivities of the double bond caused by the ethylidene and vinyl groups. The N-terminal conserved Cys of Bph covalently ligates $C3^2$, which in the free state of BV forms a double bond with $C3^1$. Conversely, PCB has a double bond between $C3^1$ and C3 and covalently ligates the conserved Cys within the GAF domain of Cph1 and CBCRs via $C3^1$. Because there have been no reports that a Cys within a CBCR GAF domain covalently ligates BV, it is difficult to predict whether the covalent bonding site of the ring A to Cys304 is $C3^1$ or $C3^2$. However, based on the AnPixJg2 structure, Cys304 is more likely to be physically near $C3^1$ of BV rather than $C3^2$, suggesting that $C3^1$ is involved in the covalent bond (Fig. S5). On the other hand, red/green CBCR, AnPixJg2, did not bind BV[8]. For those GAF domains, a different orientation of the ring D may control chromophore binding, i.e., the BV C18 ethylidene of ring D may sterically interfere with BV binding, whereas such steric hindrance in AM1_1557g2 may be absent because the local environment surrounding ring D is different. In this context, residues unique to AM1_1557g2 surrounding ring D would be possible determinants for chromophore selectivity. Although we could not detect obvious differences in residues that directly interact with ring D among AM1_1557g2 and the other red/green CBCRs, notably, AnPixJg2 Asn354 that is within van der Waals distance of Tyr352 (Tyr335 in AM1_1557g2) (Fig. S5), which interacts with the ring D carbonyl, is replaced with a Leu in AM1_1557g2 (Leu337, Fig. S1). This replacement may affect the position of Tyr335, resulting in a different arrangement of ring D within its binding pocket. To examine role of Leu337 in the chromophore selectivity, we replaced Leu337 with an Asn to form AM1_1557g2_L337N. As a result, binding efficiency of L337N to BV was approximately half of that of the wild type protein, whereas binding efficiencies of L337N and wild type proteins to PCB were almost same (Fig. 2 and Fig. S8). This result indicates that Leu337 is a major factor for potential to bind BV. The L337N protein still retains a potential to ligate BV. Additional residues may also be involved in chromophore selectivity.

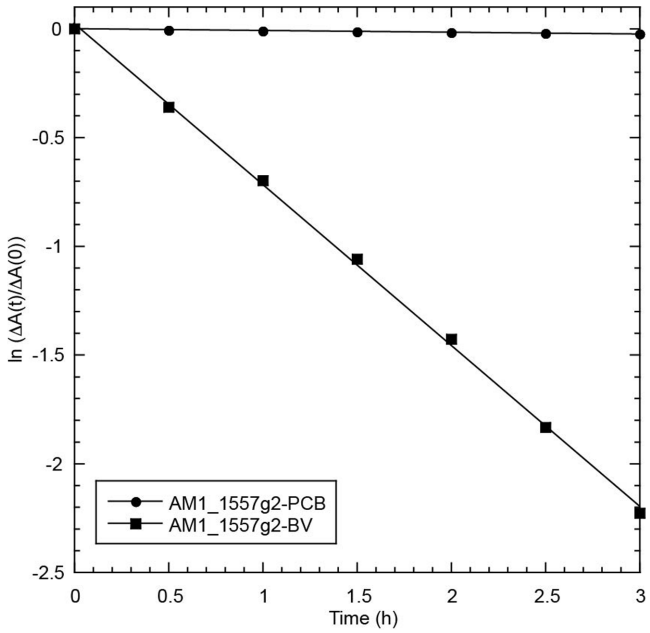

Figure 4 | Dark reversion kinetics of Pr and Pfr forms of AM1_1557g2-PCB and AM1_1557g2-BV, respectively, at room temperature. Absorbances at 649 nm and 696 nm were monitored for AM1_1557g2-PCB and AM1_1557g2-BV, respectively.

This study clearly demonstrated that AM1_1557g2 Cys304 can covalently ligate BV as well as PCB, suggesting that BV may also bind AM1_1557 *in vivo*. If such a protein exists *in vivo*, it would sense far-red light, which is more efficiently absorbed by Chl *d* than by Chl *a*. Notably, the effect of far-red light on the physiology of *A.*

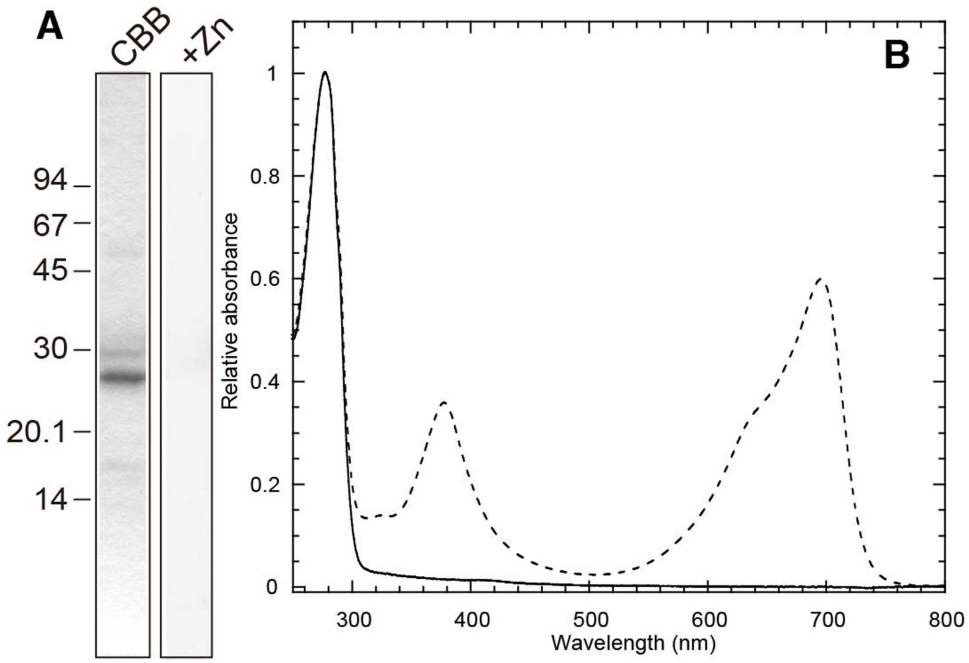

Figure 5 | Replacement of Cys304 with Ala in AM1_1557g2. (*A*) CBB-stained C304A after SDS-PAGE (CBB) and in-gel Zn-dependent fluorescence assay (+Zn) showing C304A does not bind BV. (*B*) Absorption spectra of AM1_1557g2-BV Pfr (broken line) and C304A (solid line).

marina has been studied[42,43]. Kiss et al. reported that expression of *psbE2* and *psbD3*, extra copy genes for photosystem II unique to *A. marina*, is induced under far-red light (720 nm)[42]. *A. marina* MBIC11017 accumulates phycobilisome under orange light irradiation (625 nm), but downregulates phycobiliprotein expression under far-red light irradiation (720 nm)[43]. These far-red light–inducible and far-red/orange light–reversible photo-acclimation processes are compatible with the far-red/orange photoconversion property of AM1_1557g2-BV, suggesting that AM1_1557g2-BV may be involved in such photo-acclimation process(es).

Photoconvertible and fluorescent proteins are useful tools for studying the regulation of various cell activities and monitoring/quantifying protein dynamics using optogenetic and bio-imaging techniques, respectively[34,35,44,45]. Studying the regulation of and visu-

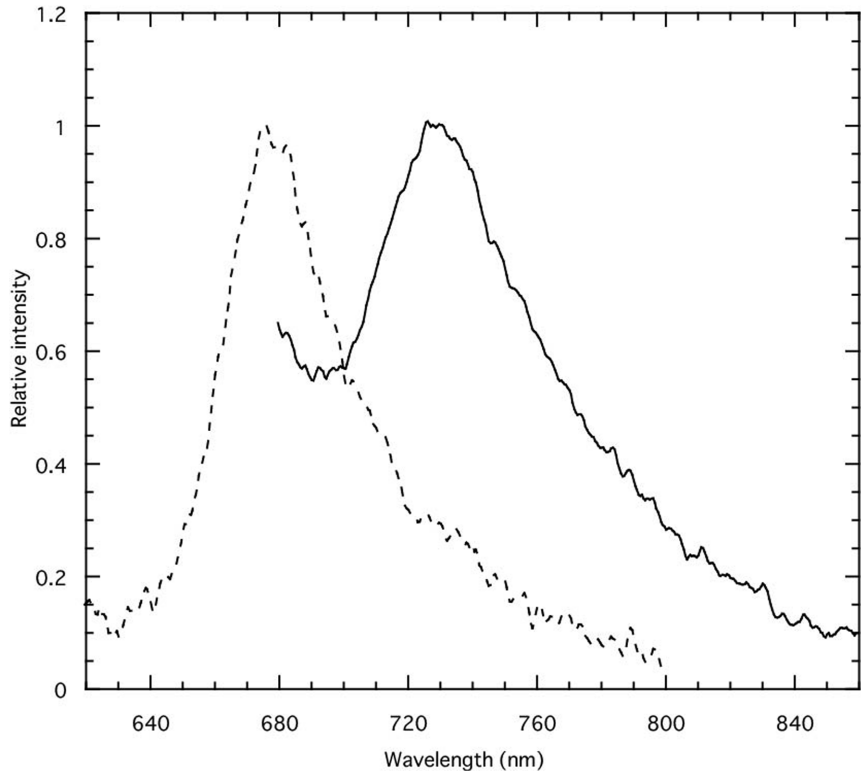

Figure 6 | Fluorescence spectra of AM1_1557g2-PCB Pr (broken line) and AM1_1557g2-BV Pfr (solid line). Excitation maxima: 590 and 660 nm, respectively.

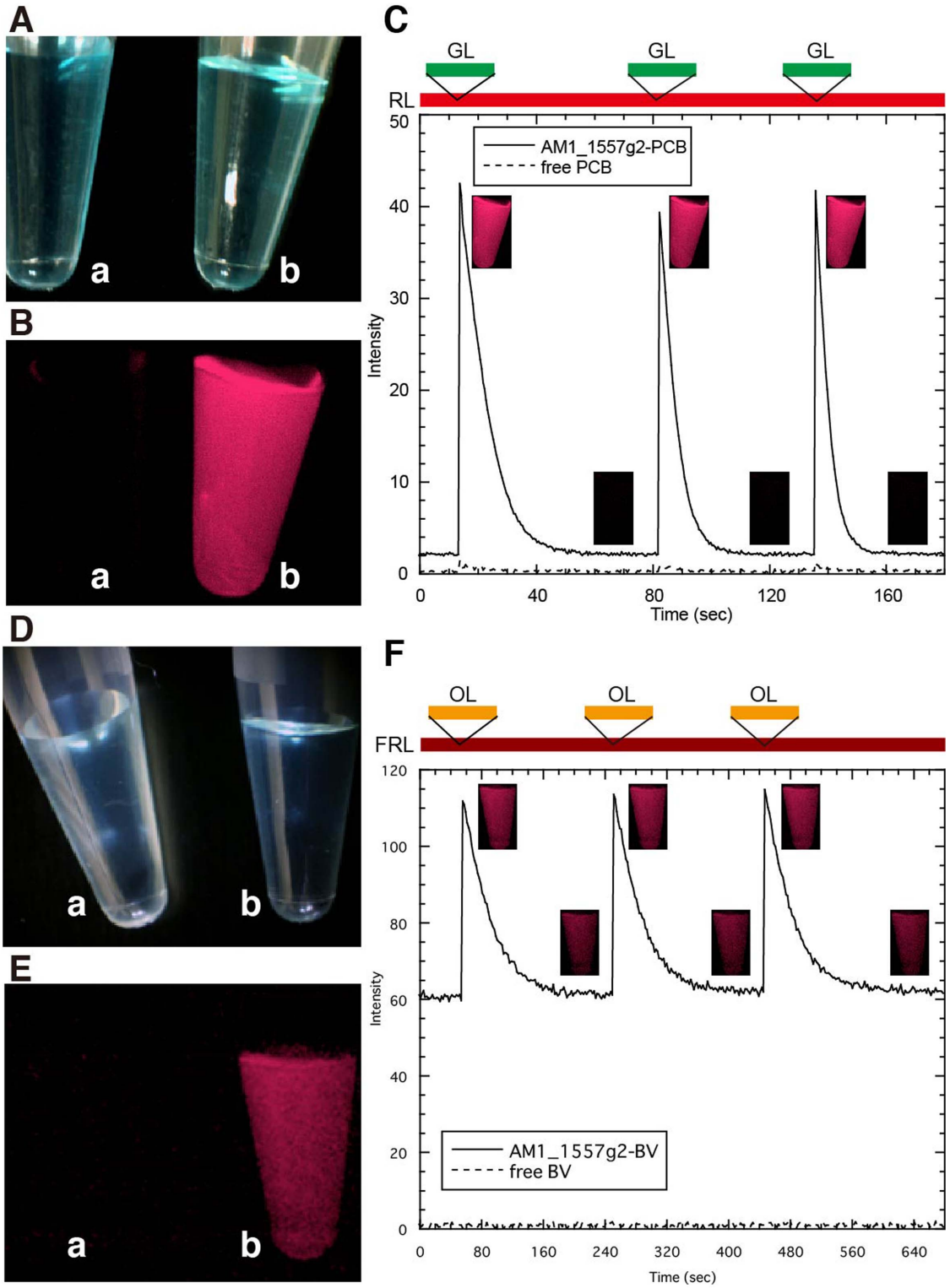

Figure 7 | Fluorescent microscopy. (*A*) Transmission and (*B*) fluorescence images of solutions of (a) free PCB and (b) AM1_1557g2-PCB. PCB was obtained from Frontier Scientific. As a control, 50 μM PCB in Buffer A was used. (*C*) Change in fluorescent intensity of AM1_1557g2-PCB during (Pr – Pg) photoconversion. Fluorescence from Pr was detected when AM1_1557g2-PCB was irradiated with red light (RL). Red-light irradiation was continuous throughout the experiment. Photoconversion was induced by intermittent green light (GL) irradiation. The fluorescence intensities of AM1_1557g2-PCB and free PCB are plotted against time. (*D*) Transmission and (*E*) fluorescence images of solutions of (a) free BV and (b) AM1_1557g2-BV. BV was obtained from Frontier Scientific. As a control, 50 μM BV in Buffer A was used. (*F*) Change in the fluorescent intensity of AM1_1557g2-BV during (Pfr – Po) photoconversion. Fluorescence from Pfr was detected when AM1_1557g2-BV was irradiated with far-red light (FRL). Far-red light irradiation was continuous throughout the experiment. Photoconversion was induced by intermittent orange-light (OL) irradiation. The fluorescence intensities of AM1_1557g2-BV and free BV are plotted against time.

alizing deep tissues in mammals using GFPs and rhodopsins are problematic because the absorbance of hemoglobin and skin melanin interferes with the analyses. Instead, proteins that can be used for these purposes should have absorption maxima within the far-red to the near-infrared spectral region (650∼900 nm), as light absorbance within this region by mammalian tissues is negligible. Consequently, red/far-red light responsive phytochromes have been used for these purposes[35,46–48]. Among various phytochromes, BV-binding Bphs have been studied for their potential as optogenetic and bio-imaging tools because BV is present in mammalian cells and absorbs light of the longest wavelengths found for linear tetrapyrrole molecules[46,47,49]. BV-binding Bphs, however, have drawbacks as their chromophore-binding unit consisting of the three domains is large and as they have a tendency to polymerize[46]. Conversely, CBCRs have the advantage of having a compact chromophore-binding unit composed of only a GAF domain (25 kDa) and do not polymerize[25]. Further, BV-binding CBCR GAF domain discovered in this study provides large advantages for application in animal deep tissues.

Because the light signals acquired by CBCR GAF domains are transferred to their enzymatic domains, e.g., the His kinase domain of AM1_1557, optogenetic switches can be created by fusing an input AM1_1557 GAF domain and an enzymatic domain. Detection of clear isosbestic points in the spectrum of AM1_1557g2-BV during photoconversion and its ability to repetitively and reversibly photoconvert without appreciable deterioration of its spectra ensure its reliable performance as a photoconvertible switch.

AM1_1557g2-BV Pfr emits fluorescence with a maximum at 730 nm, which is a wavelength comparable with or slightly longer than those of Bph-derived iRFP (near-infrared fluorescent probe) and IFP (infrared fluorescent protein)[46,47,50]. Further, the repetitive photoconversion do not affect its fluorescent properties (Fig. 7). These characteristics may be advantageous for super-resolution imaging[51]. AM1_1557g2-BV as a fluorescent probe may also be useful for plant-cell studies. Plants possess a large quantity of Chl *a* that absorbs red light and emit light at ∼680 nm, which would largely interfere with a red light–absorbing optogenetic switch or bio-imaging probe. Conversely, the far-red light–absorbing property of AM1_1557g2-BV would be immune to the spectral properties of Chl. The quantum yield of Pfr form of AM1_1557g2-BV is not so high (0.3%), but is comparable to those of the native phytochromes[52]. In the case of phytochromes, random and site-directed mutagenesis succeeded in elevating the quantum yields to 5–10%[46,47] and so we would expect similar improvement of AM1_1557g2-BV by introducing replacements of amino acid residues. The crystal structure of AnPixJg2 Pr has been solved, which enables further development and improvement of BV-binding CBCRs. So, based on this structural information, we are now performing further analyses such as mutagenesis for stable and bright fluorescence probes and chimeric protein construction for useful light switches.

Methods

***In silico* Characterization of AM1_1557.** The domain composition of AM1_1557 was determined using SMART (http://smart.embl-heidelberg.de/)[53]. Alignment and phylogenetic clustering of CBCR and phytochrome GAF domain sequences were performed by CLUSTAL_X[54]. The alignment was then modified by hand. The phylogenetic tree was drawn by Dendroscope[55].

Plasmid Construction. The nucleotide sequence of AM1_1557g2 was cloned into pET28a (Novagen) using the In-Fusion HD Cloning kit (TaKaRa). The DNA fragment corresponding to *AM1_1557g2* was PCR amplified using the synthetic primers 5′-CGCGGCAGCCATATGTATGAGCGTAATATTGCT-3′ (forward primer) and 5′-CTCGAATTCGGATCCTCATGCTTCTGCTTTATCTCT-3′ (reverse primer), genomic DNA from *A. marina* MBIC11017, and PrimeSTAR Max DNA polymerase. pET28a was PCR amplified using the synthetic primers 5′-CATATGGCTGCCGCGCGG-3′ (forward primer) and 5′-GGATCCGAATTCGAGCTC-3′ (reverse primer), pET28a, and PrimeSTAR Max DNA polymerase. A plasmid expressing AM1_1557g2 (pET28a_AM1_1557g2) was then constructed with the TaKaRa in-fusion system reagents. pET28a_AM1_1557g2_C304A was generated using the primers 5′-AGAGACGCACATTTAGAGATTTTGGAA-3′ (forward primer) and 5′-TAAATGTGCGTCTCTATAAGATTCTTG-3′ (reverse primer), pET28a_AM1_1557g2, and PrimeSTAR Max Basal Mutagenesis kit reagents (TaKaRa). pET28a_AM1_1557g2_L337N was obtained in the same way as described above with a primer set (5′- CTATCAGAATAACGTCCCACGTCAATG-3′, 5′-ACGTTATTCTGATAGGCTGCCAGCAA-3′). The sequences of the genes encoding AM1_1557g2, C304A and L337N were verified by DNA sequencing.

Expression and Purification of His-tagged AM1_1557g2, C304A and L337N. *E. coli* C41 (Novagen) carrying pKT270 or pKT271[56] was used for expression of AM1_1557g2, C304A and L337N. Each culture was incubated at 37°C for 2.5 h in 1 L of Luria-Bertani medium, 20 μg ml^{-1} kanamycin, and 20 μg ml^{-1} chloramphenicol, after which isopropyl-thio-β-D-galactopyranoside was added (final concentration, 0.1 mM). Cells were then cultured at 18°C overnight, after which they were harvested by centrifugation, frozen at −80°C, thawed at 4°C, and suspended in 50 ml of Buffer A (20 mM HEPES-NaOH, pH 7.5, 100 mM NaCl, 10% (w/v) glycerol). Cells were disrupted by three passages through an Emulsiflex C5 high-pressure homogenizer at 12,000 psi (Avestin). The cell extract was centrifuged at 109,200 × *g* for 30 min at 4°C. Each supernatant was individually passed through a nickel-affinity His-trap chelating column (GE Healthcare). After washing the column with Buffer A containing 30 mM imidazole, His-labeled proteins were eluted using a step gradient of 50, 100, and 200 mM imidazole in Buffer A. Most His-tagged proteins were recovered in the 200-mM imidazole fraction, which was studied after removal of imidazole by dialysis against Buffer A.

SDS-PAGE and Zn-induced Fluorescence Assay. Proteins in 2% (w/v) lithium dodecylsulfate, 60 mM DTT, 60 mM Tris-HCl, pH 8.0 were subjected to SDS-PAGE (15% (w/v) acrylamide), followed by staining with Coomassie Brilliant Blue R-250. For the Zn-induced fluorescence assay, after SDS-PAGE, the gel was soaked in 20 μM zinc acetate at room temperature for 30 min[57]. Then, fluorescence was visualized through a 605 nm filter upon excitation at 532 nm (FMBIO II; Takara).

Spectroscopy. Ultraviolet and visible absorption spectra of the proteins were recorded with a Shimadzu UV-2600 spectrophotometer at room temperature. Monochromic light of various wavelengths was generated using a variable wavelength light source (Opto-Spectrum Generator, Hamamatsu Photonics, Inc.). After denaturing the proteins in 8 M urea, pH 2.0 under the dark condition, their absorption spectra were recorded. Then, the protein samples were irradiated with white light for 3 min, and absorption spectra were again recorded. Fluorescence spectra of AM1_1557g2-BV Po and Pfr were recorded with a StellarNet SILVER-Nova spectrometer. Fluorescence quantum yields were measured with Quantaurus-QY (Hamamatsu Photonics).

Fluorescence Imaging. Fluorescence images of purified AM1_1557g2-PCB were acquired using a macro zoom fluorescence microscope (MVX10, Olympus) equipped with a cooled CCD camera (Rolera-XR Fast 1394, Q-imaging) and a Cy5.5 filter set (Cy5.5-B-000, Semrock). The CCD camera was controlled by MetaMorph software (Molecular Devices). Upon excitation of AM1_1557g2-PCB at 655/40 nm, fluorescence images were obtained through the 716/40 nm filter. Time lapse sequences were acquired at 1 s intervals with exposure time of 20 ms. For photoconversion from Pg to Pr form of AM1_1557g2-PCB, green light was applied using the variable wavelength light source (510/40 nm, 10%, 50-110 s). To acquire a transmitted image, the CCD camera was replaced with a digital camera (EOS Kiss, Canon).

Fluorescence images of purified AM1_1557g2-BV were acquired using a fluorescence stereomicroscope (M205A, Leica) equipped with a Cy7 filter set (ET Cy7, Leica) and the cooled CCD camera Rolera-XR Fast 1394 controlled by MetaMorph software. Upon excitation of AM1_1557g2-BV at 710/75 nm, fluorescence images were obtained through the 810/90 nm filter. Time lapse sequences were acquired at 2 s intervals with exposure time of 750 ms. For photoconversion from Po to Pfr form of AM1_1557g2-BV, orange light was applied by the variable wavelength light source (590/40 nm, 100%, 35 s). For photoconversion from Pfr to Po form of AM1_1557g2-BV, far-red light was applied using the variable wavelength light source (720/40 nm, 100%, 35 s). A transmitted image was acquired with the digital camera EOS Kiss.

1. Narikawa, R., Enomoto, G., Ni Ni, W., Fushimi, K. & Ikeuchi, M. A new type of dual-Cys cyanobacteriochrome GAF domain found in cyanobacterium *Acaryochloris marina*, which has an unusual red/blue reversible photoconversion cycle. *Biochemistry* **53**, 5051–5059, doi:10.1021/bi500376b (2014).
2. Rockwell, N. C., Martin, S. S. & Lagarias, J. C. Red/Green cyanobacteriochromes: sensors of color and power. *Biochemistry* **51**, 9667–9677, doi:10.1021/bi3013565 (2012).
3. Rockwell, N. C., Martin, S. S. & Lagarias, J. C. Mechanistic insight into the photosensory versatility of DXCF cyanobacteriochromes. *Biochemistry* **51**, 3576–3585, doi:10.1021/bi300171s (2012).
4. Rockwell, N. C., Martin, S. S., Gulevich, A. G. & Lagarias, J. C. Phycoviolobilin formation and spectral tuning in the DXCF cyanobacteriochrome subfamily. *Biochemistry* **51**, 1449–1463, doi:10.1021/bi201783j (2012).
5. Narikawa, R. *et al*. Novel photosensory two-component system (PixA-NixB-NixC) involved in the regulation of positive and negative phototaxis of cyanobacterium *Synechocystis* sp. PCC 6803. *Plant Cell Physiol.* **52**, 2214–2224, doi:10.1093/pcp/pcr155 (2011).

6. Rockwell, N. C. *et al*. A second conserved GAF domain cysteine is required for the blue/green photoreversibility of cyanobacteriochrome Tlr0924 from *Thermosynechococcus elongatus*. *Biochemistry* **47**, 7304–7316, doi:10.1021/bi800088t (2008).
7. Narikawa, R., Kohchi, T. & Ikeuchi, M. Characterization of the photoactive GAF domain of the CikA homolog (SyCikA, Slr1969) of the cyanobacterium *Synechocystis* sp. PCC 6803. *Photochem. Photobiol. Sci.* **7**, 1253–1259, doi:10.1039/b811214b (2008).
8. Narikawa, R., Fukushima, Y., Ishizuka, T., Itoh, S. & Ikeuchi, M. A novel photoactive GAF domain of cyanobacteriochrome AnPixJ that shows reversible green/red photoconversion. *J. Mol. Biol.* **380**, 844–855, doi:10.1016/j.jmb.2008.05.035 (2008).
9. Hirose, Y., Shimada, T., Narikawa, R., Katayama, M. & Ikeuchi, M. Cyanobacteriochrome CcaS is the green light receptor that induces the expression of phycobilisome linker protein. *Proc. Natl. Acad. Sci. U. S. A.* **105**, 9528–9533 (2008).
10. Ishizuka, T. *et al*. Characterization of cyanobacteriochrome TePixJ from a thermophilic cyanobacterium *Thermosynechococcus elongatus* strain BP-1. *Plant Cell Physiol.* **47**, 1251–1261 (2006).
11. Yoshihara, S., Katayama, M., Geng, X. & Ikeuchi, M. Cyanobacterial phytochrome-like PixJ1 holoprotein shows novel reversible photoconversion between blue- and green-absorbing forms. *Plant Cell Physiol.* **45**, 1729–1737 (2004).
12. Ma, Q. *et al*. A rising tide of blue-absorbing biliprotein photoreceptors: characterization of seven such bilin-binding GAF domains in *Nostoc* sp. PCC7120. *FEBS J.* **279**, 4095–4108, doi:10.1111/febs.12003 (2012).
13. Savakis, P. *et al*. Light-induced alteration of c-di-GMP level controls motility of *Synechocystis* sp. PCC 6803. *Mol. Microbiol.* **85**, 239–251, doi:10.1111/j.1365-2958.2012.08106.x (2012).
14. Song, J. Y. *et al*. Near-UV cyanobacteriochrome signaling system elicits negative phototaxis in the cyanobacterium *Synechocystis* sp. PCC 6803. *Proc. Natl. Acad. Sci. U. S. A.* **108**, 10780–10785, doi:10.1073/pnas.1104242108 (2011).
15. Hirose, Y., Narikawa, R., Katayama, M. & Ikeuchi, M. Cyanobacteriochrome CcaS regulates phycoerythrin accumulation in *Nostoc punctiforme*, a group II chromatic adapter. *Proc. Natl. Acad. Sci. U. S. A.* **107**, 8854–8859, doi:10.1073/pnas.1000177107 (2010).
16. Enomoto, G. *et al*. Cyanobacteriochrome SesA is a diguanylate cyclase that induces cell aggregation in *Thermosynechococcus*. *J. Biol. Chem.* **289**, 24801–24809, doi:10.1074/jbc.M114.583674 (2014).
17. Rockwell, N. C., Martin, S. S., Feoktistova, K. & Lagarias, J. C. Diverse two-cysteine photocycles in phytochromes and cyanobacteriochromes. *Proc. Natl. Acad. Sci. U. S. A.* **108**, 11854–11859, doi:10.1073/pnas.1107844108 (2011).
18. Ishizuka, T. *et al*. The cyanobacteriochrome, TePixJ, isomerizes its own chromophore by converting phycocyanobilin to phycoviolobilin. *Biochemistry* **50**, 953–961, doi:10.1021/bi101626t (2011).
19. Hirose, Y. *et al*. Green/red cyanobacteriochromes regulate complementary chromatic acclimation via a protochromic photocycle. *Proc. Natl. Acad. Sci. U. S. A.* **110**, 4974–4979, doi:10.1073/pnas.1302909110 (2013).
20. Chen, Y. *et al*. Photophysical diversity of two novel cyanobacteriochromes with phycocyanobilin chromophores: photochemistry and dark reversion kinetics. *FEBS J.* **279**, 40–54, doi:10.1111/j.1742-4658.2011.08397.x (2012).
21. Kim, P. W. *et al*. Second-chance forward isomerization dynamics of the red/green cyanobacteriochrome NpR6012g4 from *Nostoc punctiforme*. *J. Am. Chem. Soc.* **134**, 130–133, doi:10.1021/ja209533x (2011).
22. Kim, P. W. *et al*. Femtosecond photodynamics of the red/green cyanobacteriochrome NpR6012g4 from *Nostoc punctiforme*. 1. Forward dynamics. *Biochemistry* **51**, 608–618, doi:10.1021/bi201507k (2011).
23. Kim, P. W. *et al*. Femtosecond photodynamics of the red/green cyanobacteriochrome NpR6012g4 from *Nostoc punctiforme*. 2. reverse dynamics. *Biochemistry* **51**, 619–630, doi:10.1021/bi2017365 (2011).
24. Fukushima, Y. *et al*. Photoconversion mechanism of a green/red photosensory cyanobacteriochrome AnPixJ: time-resolved optical spectroscopy and FTIR analysis of the AnPixJ-GAF2 domain. *Biochemistry* **50**, 6328–6339, doi:10.1021/bi101799w (2011).
25. Narikawa, R. *et al*. Structures of cyanobacteriochromes from phototaxis regulators AnPixJ and TePixJ reveal general and specific photoconversion mechanism. *Proc. Natl. Acad. Sci. U. S. A.* **110**, 918–923, doi:10.1073/pnas.1212098110 (2013).
26. Narikawa, R., Muraki, N., Shiba, T., Ikeuchi, M. & Kurisu, G. Crystallization and preliminary X-ray studies of the chromophore-binding domain of cyanobacteriochrome AnPixJ from *Anabaena* sp. PCC 7120. *Acta Crystallogr. Sect. F Struct. Biol. Cryst. Commun.* **65**, 159–162, doi:10.1107/S1744309108044151 (2009).
27. Velazquez Escobar, F. *et al*. Photoconversion Mechanism of the Second GAF Domain of Cyanobacteriochrome AnPixJ and the Cofactor Structure of Its Green-Absorbing State. *Biochemistry* **52**, 4871–4880, doi:10.1021/bi400506a (2013).
28. Loughlin, P., Lin, Y. & Chen, M. Chlorophyll d and *Acaryochloris marina*: current status. *Photosynth. Res.* **116**, 277–293, doi:10.1007/s11120-013-9829-y (2013).
29. Tomo, T., Allakhverdiev, S. I. & Mimuro, M. Constitution and energetics of photosystem I and photosystem II in the chlorophyll *d*-dominated cyanobacterium *Acaryochloris marina*. *J. Photochem. Photobiol. B* **104**, 333–340, doi:10.1016/j.jphotobiol.2011.02.017 (2011).
30. Hu, Q. *et al*. A photosystem I reaction center driven by chlorophyll d in oxygenic photosynthesis. *Proc. Natl. Acad. Sci. U. S. A.* **95**, 13319–13323 (1998).
31. Tomo, T. *et al*. Identification of the special pair of photosystem II in a chlorophyll d-dominated cyanobacterium. *Proc. Natl. Acad. Sci. U. S. A.* **104**, 7283–7288, doi:10.1073/pnas.0701847104 (2007).
32. Chen, M., Bibby, T. S., Nield, J., Larkum, A. & Barber, J. Iron deficiency induces a chlorophyll d-binding Pcb antenna system around Photosystem I in *Acaryochloris marina*. *Biochim. Biophys. Acta* **1708**, 367–374, doi:10.1016/j.bbabio.2005.05.007 (2005).
33. Swingley, W. D. *et al*. Niche adaptation and genome expansion in the chlorophyll d-producing cyanobacterium *Acaryochloris marina*. *Proc. Natl. Acad. Sci. U. S. A.* **105**, 2005–2010, doi:10.1073/pnas.0709772105 (2008).
34. Sato, M. Genetically encoded fluorescent biosensors for live cell imaging of lipid dynamics. *Methods Mol. Biol.* **1071**, 73–81, doi:10.1007/978-1-62703-622-1_6 (2014).
35. Shcherbakova, D. M., Subach, O. M. & Verkhusha, V. V. Red fluorescent proteins: advanced imaging applications and future design. *Angew. Chem. Int. Ed. Engl.* **51**, 10724–10738, doi:10.1002/anie.201200408 (2012).
36. Auldridge, M. E. & Forest, K. T. Bacterial phytochromes: more than meets the light. *Crit. Rev. Biochem. Mol. Biol.* **46**, 67–88, doi:10.3109/10409238.2010.546389 (2011).
37. Ikeuchi, M. & Ishizuka, T. Cyanobacteriochromes: a new superfamily of tetrapyrrole-binding photoreceptors in cyanobacteria. *Photochem. Photobiol. Sci.* **7**, 1159–1167, doi:10.1039/b802660m (2008).
38. Lamparter, T., Michael, N., Mittmann, F. & Esteban, B. Phytochrome from *Agrobacterium tumefaciens* has unusual spectral properties and reveals an N-terminal chromophore attachment site. *Proc. Natl. Acad. Sci. U. S. A.* **99**, 11628–11633 (2002).
39. Yang, X., Kuk, J. & Moffat, K. Conformational differences between the Pfr and Pr states in *Pseudomonas aeruginosa* bacteriophytochrome. *Proc. Natl. Acad. Sci. U. S. A.* **106**, 15639–15644, doi:10.1073/pnas.0902178106 (2009).
40. Wagner, J. R., Brunzelle, J. S., Forest, K. T. & Vierstra, R. D. A light-sensing knot revealed by the structure of the chromophore-binding domain of phytochrome. *Nature* **438**, 325–331 (2005).
41. Essen, L. O., Mailliet, J. & Hughes, J. The structure of a complete phytochrome sensory module in the Pr ground state. *Proc. Natl. Acad. Sci. U. S. A.* **105**, 14709–14714, doi:10.1073/pnas.0806477105 (2008).
42. Kiss, E., Kos, P. B., Chen, M. & Vass, I. A unique regulation of the expression of the *psbA*, *psbD*, and *psbE* genes, encoding the D1, D2 and cytochrome b559 subunits of the Photosystem II complex in the chlorophyll *d* containing cyanobacterium *Acaryochloris marina*. *Biochim. Biophys. Acta* **1817**, 1083–1094, doi:10.1016/j.bbabio.2012.04.010 (2012).
43. Duxbury, Z., Schliep, M., Ritchie, R. J., Larkum, A. W. & Chen, M. Chromatic photoacclimation extends utilisable photosynthetically active radiation in the chlorophyll d-containing cyanobacterium, *Acaryochloris marina*. *Photosynth. Res.* **101**, 69–75, doi:10.1007/s11120-009-9466-7 (2009).
44. Moglich, A. & Moffat, K. Engineered photoreceptors as novel optogenetic tools. *Photochem. Photobiol. Sci.* **9**, 1286–1300, doi:10.1039/c0pp00167h (2010).
45. Stepanenko, O. V., Stepanenko, O. V., Kuznetsova, I. M., Verkhusha, V. V. & Turoverov, K. K. Beta-barrel scaffold of fluorescent proteins: folding, stability and role in chromophore formation. *Int. Rev. Cell Mol. Biol.* **302**, 221–278, doi:10.1016/b978-0-12-407699-0.00004-2 (2013).
46. Filonov, G. S. *et al*. Bright and stable near-infrared fluorescent protein for in vivo imaging. *Nat. Biotechnol.* **29**, 757–761, doi:10.1038/nbt.1918 (2011).
47. Shu, X. *et al*. Mammalian expression of infrared fluorescent proteins engineered from a bacterial phytochrome. *Science* **324**, 804–807, doi:10.1126/science.1168683 (2009).
48. Leung, D. W., Otomo, C., Chory, J. & Rosen, M. K. Genetically encoded photoswitching of actin assembly through the Cdc42-WASP-Arp2/3 complex pathway. *Proc. Natl. Acad. Sci. U. S. A.* **105**, 12797–12802, doi:10.1073/pnas.0801232105 (2008).
49. Filonov, G. S. & Verkhusha, V. V. A near-infrared BiFC reporter for in vivo imaging of protein-protein interactions. *Chem. Biol.* **20**, 1078–1086, doi:10.1016/j.chembiol.2013.06.009 (2013).
50. Yu, D. *et al*. An improved monomeric infrared fluorescent protein for neuronal and tumour brain imaging. *Nat. Commun.* **5**, 3626, doi:10.1038/ncomms4626 (2014).
51. Chozinski, T. J., Gagnon, L. A. & Vaughan, J. C. Twinkle, twinkle little star: Photoswitchable fluorophores for super-resolution imaging. *FEBS Lett.* **588**, 3603–3612, doi:10.1016/j.febslet.2014.06.043 (2014).
52. Sineshchekov, V. Photobiophysics and photobiochemistry of the heterogenous phytochrome system. *Biochim. Biophys. Acta* **1228**, 125–164 (1995).
53. Schultz, J., Milpetz, F., Bork, P. & Ponting, C. P. SMART, a simple modular architecture research tool: identification of signaling domains. *Proc. Natl. Acad. Sci. U. S. A.* **95**, 5857–5864 (1998).
54. Thompson, J. D., Gibson, T. J., Plewniak, F., Jeanmougin, F. & Higgins, D. G. The CLUSTAL_X windows interface: flexible strategies for multiple sequence alignment aided by quality analysis tools. *Nucleic Acids Res.* **25**, 4876–4882 (1997).
55. Huson, D. H. *et al*. Dendroscope: An interactive viewer for large phylogenetic trees. *BMC Bioinformatics* **8**, 460, doi:10.1186/1471-2105-8-460 (2007).
56. Mukougawa, K., Kanamoto, H., Kobayashi, T., Yokota, A. & Kohchi, T. Metabolic engineering to produce phytochromes with phytochromobilin, phycocyanobilin,

or phycoerythrobilin chromophore in *Escherichia coli*. *FEBS Lett.* **580**, 1333–1338 (2006).
57. Berkelman, T. R. & Lagarias, J. C. Visualization of bilin-linked peptides and proteins in polyacrylamide gels. *Anal. Biochem.* **156**, 194–201 (1986).

Acknowledgments

We thank Dr. Nathan C. Rockwell for helpful discussion and kind reading of the manuscript. This work was supported by Precursory Research for Embryonic Science and Technology, Japan Science and Technology Agency, 4-1-8 Honcho Kawaguchi, Saitama 332-0012 (to R.N.) and Grants-in-Aid for Young Scientists (to R.N.).

Author contributions

R.N., M.S. and M.I. designed the research. R.N., N.N.W. and K.F. prepared plasmids for expression of AM1_1557g2. R.N. purified AM1_1557g2 proteins and performed spectroscopic analyses. G.E. performed purification and spectroscopic analysis of PaBphP. R.N., T.N., Y.A. and S.I. detected fluorescence from AM1_1557g2. R.N., M.S. and M.I. analyzed the data and wrote the manuscript.

Additional information

Supplementary information accompanies this paper at http://www.nature.com/scientificreports

Competing financial interests: The authors declare no competing financial interests.

How to cite this article: Narikawa, R. *et al*. A biliverdin-binding cyanobacteriochrome from the chlorophyll *d*–bearing cyanobacterium *Acaryochloris marina*. *Sci. Rep.* **5**, 7950; DOI:10.1038/srep07950 (2015).